Inorg. Chem. **2008**, *47*, 9303−9313

Neglected Bidentate sp^2 N-Donor Carrier Ligands with Triazine Nitrogen Lone Pairs: Platinum Complexes Retromodeling Cisplatin Guanine Nucleobase Adducts

Vidhi Maheshwari, Patricia A. Marzilli, and Luigi G. Marzilli*

Department of Chemistry, Louisiana State University, Baton Rouge, Louisiana 70803

Received May 7, 2008

Rapid rotation of guanine base derivatives about Pt−N7 bonds results in fluxional behavior of models of the key DNA intrastrand G−G cross-link leading to anticancer activity of Pt(II) drugs (G = deoxyguanosine). This behavior impedes the characterization of **L**Pt**G**$_2$ models (**L** = one bidentate or two *cis*-unidentate carrier ligands; **G** = guanine derivative not linked by a phosphodiester group). We have examined the formation of **L**Pt**G**$_2$ adducts with **G** = 5′- and 3′-GMP and **L** = sp^2 N-donor bidentate carrier ligands [5,5′-dimethyl-2,2′-bipyridine (**5,5′-Me$_2$bipy**), 3-(4′-methylpyridin-2′-yl)-5,6-dimethyl-1,2,4-triazine) (**MepyMe$_2$t**), and bis-3,3′-(5,6-dialkyl-1,2,4-triazine) (**R$_4$dt**)]. NMR spectroscopy provided conclusive evidence that these **L**Pt(5′-GMP)$_2$ complexes exist as interconverting mixtures of head-to-tail (HT) and head-to-head (HH) conformers. For a given **G**, the rates of **G** base rotation about the Pt−N7 bonds of **L**Pt**G**$_2$ models decrease in the order **Me$_4$dt** > **Et$_4$dt** > **MepyMe$_2$t** > **5,5′-Me$_2$bipy**. This order reveals that the pyridyl ring C6 atom + H atom grouping is large enough to impede the rotation, but the equivalently placed triazine ring N atom + N lone pair grouping is sterically less impeding. For the first time, the two possible HH conformers (HHa and HHb) in the case of an unsymmetrical **L** have been identified in our study of (**MepyMe$_2$t**)Pt(5′-GMP)$_2$. Although O6−O6 clashes involving the two cis **G** bases favor the HT over the HH arrangement for most **L**Pt**G**$_2$-type complexes, the HH conformer of (**R$_4$dt**)Pt(5′-GMP)$_2$ adducts has a high abundance (∼50%). We attribute this high abundance to a reduction in O6−O6 steric clashes permitted by the overall low steric effects of **R$_4$dt** ligands. Under the reaction conditions used, 3′-GMP forms a higher abundance of the **L**Pt(GMP)$_2$ adduct than does 5′-GMP, a result attributable to more favorable second-sphere communication in the **L**Pt(3′-GMP)$_2$ adduct than in the **L**Pt(5′-GMP)$_2$ adduct.

Introduction

Cisplatin (*cis*-Pt(NH$_3$)$_2$Cl$_2$) is one of the most widely used anticancer drugs.[1,2] Cisplatin and its analogues, **L**PtX$_2$ models (**L** = one bidentate or two *cis*-unidentate N-donor carrier ligands), interact with DNA by forming a 1,2-intrastrand N7−Pt−N7 cross-link between two adjacent guanines of d(GpG) sequences in DNA.[1−6] The cross-links formed by cisplatin (and its analogues) have been investigated and identified from X-ray structures,[1,3] NMR spectroscopy,[1,3] and enzyme digestion studies.[2,3,5]

Within the cross-link adduct, hydrogen bonding between the NH$_3$ ligands of the *cis*-Pt(NH$_3$)$_2$ moiety and residues in or near the cross-link has been an important component of hypotheses concerning the modes of stabilization of distorted DNA induced by drug binding.[7−12] However, examination of an X-ray structure of a HMG-bound 16-oligomer[13] and an X-ray/NMR-derived model of a duplex 9-oligomer,[14] both of which contain an intrastrand cisplatin lesion, suggests that hydrogen-bonding interactions involving the NH$_3$ ligands are weak or even nonexistent. If the NH$_3$ ligands are replaced by **L** carrier ligands having sp^3 N atoms bearing two or more

* Author to whom correspondence should be addressed. E-mail: lmarzil@lsu.edu.

(1) Bloemink, M. J.; Reedijk, J. In *Metal Ions in Biological Systems*; Sigel, A., Sigel, H. Eds.; Marcel Dekker: New York, 1996; Vol. *32*, pp 641−685.
(2) Reedijk, J. *J. Chem. Soc., Chem. Commun.* **1996**, 801–806.
(3) Sherman, S. E.; Lippard, S. J. *Chem. Rev.* **1987**, *87*, 1153–1181.
(4) Iwamoto, M.; Mukundan, S., Jr.; Marzilli, L. G. *J. Am. Chem. Soc.* **1994**, *116*, 6238–6244.
(5) Kline, T. P.; Marzilli, L. G.; Live, D.; Zon, G. *J. Am. Chem. Soc.* **1989**, *111*, 7057–7068.
(6) Fouts, C.; Marzilli, L. G.; Byrd, R.; Summers, M. F.; Zon, G.; Shinozuka, K. *Inorg. Chem.* **1988**, *27*, 366–376.

10.1021/ic800836t CCC: $40.75
Published on Web 09/19/2008

alkyl groups, modeling with the 9-mer structure suggests that clashes will occur.[14] These results on duplex models have led to the hypothesis that the small size of the NH group, not its hydrogen-bonding ability, facilitates the anticancer activity of Pt compounds bearing multiple NH groups.[15]

A degree of uncertainty exists in defining the structure of duplexes bearing Pt drug lesions.[15,16] Relatively few X-ray structures are available,[13,15,17] and NMR characterization is hampered because the carrier ligands in cisplatin are not bulky enough to impede the rotation of N7-bound guanine about the Pt−N7 bond.[16,18] Thus, cisplatin adducts with nucleic acids and their constituents exist as a fluxional mixture of conformers, making elucidation of the structures in the solution state difficult; this complication is termed the fast dynamic motion problem.[14,16,18,19]

To overcome the fast dynamic motion problem, a retro-modeling approach can be used by introducing features in the carrier ligand to make the spectral properties more informative.[14,19−22] Retro models are essentially analogues of cisplatin with carrier ligands designed to reduce the dynamic motion by destabilizing the transition state for Pt−N7 rotation, but having bulk in or near the coordination plane, thereby allowing the coexistence of multiple conformers. In this study, we compare the **L**Pt(GMP)$_2$ (GMP = guanosine 5′-monophosphate) adducts containing the **L** depicted in Figure 1. For an **L**Pt**G**$_2$ adduct (**G** = guanine derivative not linked by a phosphodiester group), the **G** bases can have head-to-tail (HT) or head-to-head (HH) orientations (Figure 2). The untethered **G**'s normally adopt preferentially a HT orientation,[16,23] whereas the bases in d(GpG) cross-links having a sugar phosphate backbone are found most often in the HH orientation, especially when a 5′ residue is present.[6,19,24−31]

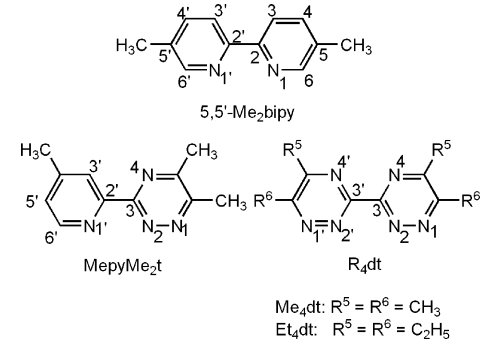

Figure 1. Line drawing and numbering scheme for 5,5′-dimethyl-2,2′-bipyridine (**5,5′-Me$_2$bipy**; top), 3-(4′-methylpyridin-2′-yl)-5,6-dimethyl-1,2,4-triazine) (**MepyMe$_2$t**; bottom left), and bis-3,3′-(5,6-dialkyl-1,2,4-triazine) (**R$_4$dt**; bottom right) ligands.

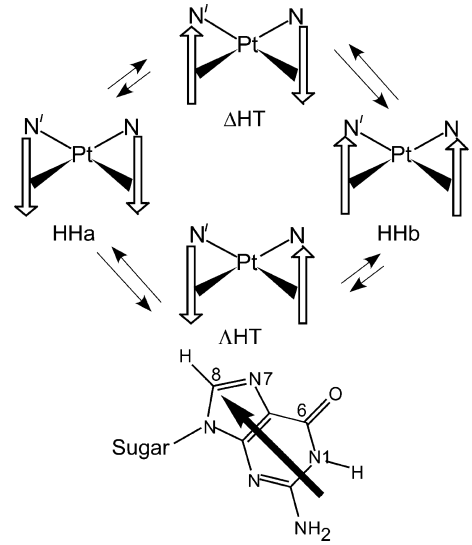

Figure 2. Possible base orientations of two cis guanine bases coordinated to Pt. Each arrow represents the base with the H8 atom at its head. In all cases, two HT conformers are possible. Two HH conformers are possible when **L** (to the rear) is unsymmetrical (N′ ≠ N, e.g., as in **MepyMe$_2$t**, N′ = pyridyl N and N = triazine N, see below), but only one HH conformer is possible when **L** is symmetrical (N′ = N). Each rotation of one base about the Pt−N7 bond leads to changes in the relative base orientation from HT to HH, or vice versa.

In order to gain a better understanding of a number of fundamental factors influencing properties of **L**Pt**G$_2$** adducts, we must know the effect of the carrier−ligand interactions with the nucleic acid constituents (bases, sugars, etc.). These interactions, present in very small adducts, also occur in

(7) Jamieson, E. R.; Lippard, S. J. *Chem. Rev.* **1999**, *99*, 2467–2498.
(8) van Garderen, C. J.; Bloemink, M. J.; Richardson, E.; Reedijk, J. *J. Inorg. Biochem.* **1991**, *42*, 199–205.
(9) Laoui, A.; Kozelka, J.; Chottard, J.-C. *Inorg. Chem.* **1988**, *27*, 2751–2753.
(10) Sherman, S. E.; Gibson, D.; Wang, A.; Lippard, S. J. *J. Am. Chem. Soc.* **1988**, *110*, 7368–7381.
(11) Farrell, N. In *Metal Ions in Biological Systems*; Sigel, A., Sigel, H. Eds.; Marcel Dekker: New York, 1996; Vol. *32*, pp 603−639.
(12) Bloemink, M. J.; Heetebrij, R. J.; Inagaki, K.; Kidani, Y.; Reedijk, J. *Inorg. Chem.* **1992**, *31*, 4656–4661.
(13) Ohndorf, U.-M.; Rould, M. A.; He, Q.; Pabo, C. O.; Lippard, S. J. *Nature (London)* **1999**, *399*, 708–712.
(14) Marzilli, L. G.; Ano, S. O.; Intini, F. P.; Natile, G. *J. Am. Chem. Soc.* **1999**, *121*, 9133–9142.
(15) Marzilli, L. G.; Saad, J. S.; Kuklenyik, Z.; Keating, K. A.; Xu, Y. *J. Am. Chem. Soc.* **2001**, *123*, 2764–2770.
(16) Ano, S. O.; Kuklenyik, Z.; Marzilli, L. G. In *Cisplatin. Chemistry and Biochemistry of a Leading Anticancer Drug*; Lippert, B. Ed.; Wiley-VCH: Weinheim, Germany, 1999; pp 247−291.
(17) Spingler, B.; Whittington, D. A.; Lippard, S. J. *Inorg. Chem.* **2001**, *40*, 5596–5602.
(18) Williams, K. M.; Cerasino, L.; Natile, G.; Marzilli, L. G. *J. Am. Chem. Soc.* **2000**, *122*, 8021–8030.
(19) Ano, S. O.; Intini, F. P.; Natile, G.; Marzilli, L. G. *Inorg. Chem.* **1999**, *38*, 2989–2999.
(20) Saad, J. S.; Scarcia, T.; Natile, G.; Marzilli, L. G. *Inorg. Chem.* **2002**, *41*, 4923–4935.
(21) Sullivan, S. T.; Ciccarese, A.; Fanizzi, F. P.; Marzilli, L. G. *Inorg. Chem.* **2000**, *39*, 836–842.
(22) Bhattacharyya, D.; Marzilli, P. A.; Marzilli, L. G. *Inorg. Chem.* **2005**, *44*, 7644–7651.
(23) Ano, S. O.; Intini, F. P.; Natile, G.; Marzilli, L. G. *J. Am. Chem. Soc.* **1997**, *119*, 8570–8571.
(24) den Hartog, J. H. J.; Altona, C.; Chottard, J.-C.; Girault, J.-P.; Lallemand, J.-Y.; de Leeuw, F. A. A. M.; Marcelis, A. T. M.; Reedijk, J. *Nucleic Acids Res.* **1982**, *10*, 4715–4730.
(25) Girault, J.-P.; Chottard, G.; Lallemand, J.-Y.; Chottard, J.-C. *Biochemistry* **1982**, *21*, 1352–1356.
(26) Kozelka, J.; Fouchet, M. H.; Chottard, J.-C. *Eur. J. Biochem.* **1992**, *205*, 895–906.
(27) Berners-Price, S. J.; Ranford, J. D.; Sadler, P. J. *Inorg. Chem.* **1994**, *33*, 584–5846.
(28) Neumann, J.-M.; Tran-Dinh, S.; Girault, J.-P.; Chottard, J.-C.; Huynh-Dinh, T. *Eur. J. Biochem.* **1984**, *141*, 465–472.
(29) Kiser, D.; Intini, F. P.; Xu, Y.; Natile, G.; Marzilli, L. G. *Inorg. Chem.* **1994**, *33*, 4149–4158.
(30) Xu, Y.; Natile, G.; Intini, F. P.; Marzilli, L. G. *J. Am. Chem. Soc.* **1990**, *112*, 8177–8179.
(31) Marzilli, L. G.; Intini, F. P.; Kiser, D.; Wong, H. C.; Ano, S. O.; Marzilli, P. A.; Natile, G. *Inorg. Chem.* **1998**, *37*, 6898–6905.

larger models, including duplexes. However, they can be more difficult to assess in the larger adducts, particularly because larger adducts manifest additional interactions involving both flanking residues in the cross-link strand and residues in the complementary strand. Retro models with sp^3 N-donor ligands have been investigated more often[16,19−21,32] than those with sp^2 N-donor heterocyclic chelating ligands. Studies of (**2,9-dimethyl-1,10-phenanthroline**)Pt(Guo)$_2$[33] (Guo = guanosine) and (**5,5′-Me$_2$bipy**)Pt(d(GpG))[22] adducts have demonstrated the coexistence of rotamers exchanging slowly relative to the NMR time scale. The (**MepyMe$_2$t**)-Pt(Guo)$_2$ adduct gave NMR evidence for rotamers, but the ease of rotation of the Guo cis to the triazine ring was difficult to assess.[34]

In cisplatin intrastrand cross-linked DNA adducts, the dominant conformer appears to have the guanines in a HH orientation.[21] For most **L**Pt**G**$_2$ adducts, the HH conformers are minor conformers, when compared to the HT conformers, and are favored more in the 5′-GMP adduct than in the corresponding 3′-GMP adduct.[19,20,30,31,35] When the **L** carrier ligand is unsymmetrical, two HH conformers are possible (Figure 2). However, in all previous work, even with the 5′-GMP adducts, it was not possible to assign the HHa and HHb conformers (Figure 2). The (**MepyMe$_2$t**)Pt(5′-GMP)$_2$ adduct studied here allowed, for the first time, the determination of the conformation of two such HH conformers. The ligands containing the triazine ring (Figure 1) have been relatively neglected (see citations in refs 34 and 36).

Experimental Section

Starting Materials. 5′-GMP, 3′-GMP (Sigma), and **5,5′-Me$_2$-bipy** (Aldrich) were used as received. *cis*-Pt(Me$_2$SO)$_2$Cl$_2$ was prepared as described in the literature.[37] The syntheses of (**5,5′-Me$_2$bipy**)PtCl$_2$ and (**MepyMe$_2$t**)PtCl$_2$ are described elsewhere.[22,34,38] Bis-3,3′-(5,6-dialkyl-1,2,4-triazine) (**R$_4$dt**, R = Me or Et) ligands were prepared by a known method[39] (Scheme 1). Elemental analyses (C,H,N) were performed by Atlantic Microlabs, Atlanta, Georgia.

NMR Measurements. ^{1}H NMR spectra were recorded on a Bruker spectrometer operating at 400 MHz. We used the values of 0.00, 4.78, and 4.98 ppm to reference signals to TMS in DMSO-d_6 solutions at 25 °C and to the residual HOD signal at 25 and 5 °C in D$_2$O/DMSO-d_6 solutions, respectively. A presaturation pulse to suppress the water peak was used when necessary. The 2D rotating-frame Overhauser enhancement spectroscopy (ROESY) experiments[40] were performed at 5 °C by using a 500 ms mixing time (128 scans per t_1 increment). ROESY and 1D NMR data, processed with the *XWINNMR* or *Mestre-C* software, were used to assign signals and (along with CD data) to assess the conformation of the adducts under various pH conditions. DNO$_3$ and NaOD solutions (0.1 M in D$_2$O) were used to adjust the pH of D$_2$O/DMSO-d_6 solutions, especially during the reactions in which the pH decreased with time.

Scheme 1. Synthesis of Bis-3,3′-(5,6-dialkyl-1,2,4-triazine) (**R$_4$dt**) Ligands

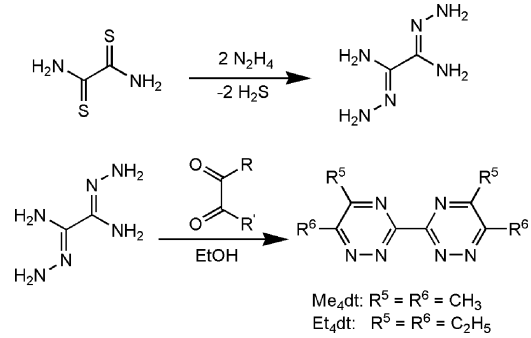

Circular Dichroism (CD) Spectroscopy. All samples used for CD experiments were prepared from the respective NMR samples by diluting to ∼0.025 mM Pt with deionized water. Spectra were recorded from 400 to 200 nm at a scan speed of 50 nm/min on a JASCO J-600 CD spectropolarimeter. Six scans were recorded and averaged for each sample.

Synthesis of (R$_4$dt)PtCl$_2$ Complexes. The (**R$_4$dt**)PtCl$_2$ complexes were obtained as yellow precipitates upon heating a methanol solution (10 mL) of *cis*-Pt(Me$_2$SO)$_2$Cl$_2$ (42.2 mg, 0.1 mmol) and the desired **R$_4$dt** ligand (0.1 mmol) at 60 °C for 6 h. The precipitates were collected, washed with diethyl ether, followed by chloroform, and then dried in vacuo.

(Me$_4$dt)PtCl$_2$. The method described above afforded a yellow precipitate; yield, 26.5 mg (55%). ^{1}H NMR (ppm) in DMSO-d_6: 2.62 (s, 5-CH$_3$), 2.81 (s, 6-CH$_3$). Anal. calcd for C$_{10}$H$_{12}$Cl$_2$N$_6$Pt·1/3(H$_2$O): C, 24.58; H, 2.59; N, 17.21. Found: C, 24.66; H, 2.69; N, 16.91.

(Et$_4$dt)PtCl$_2$. The product was obtained as a yellow powder; yield, 36.1 mg (67%). ^{1}H NMR (ppm) in DMSO-d_6: 3.20 (quartet, 6-CH$_2$), 2.96 (quartet, 5-CH$_2$), 1.30−1.41 (m, 5,6-CH$_3$). X-ray-quality crystals were obtained by mixing equal volumes of 10 mM solutions of *cis*-Pt(Me$_2$SO)$_2$Cl$_2$ (8.44 mg, 10 mM) and the **Et$_4$dt** ligand (5.44 mg) in 2 mL of acetonitrile and allowing this solution to stand at 25 °C. Thin yellow needles of (**Et$_4$dt**)PtCl$_2$ were obtained in ∼25% yield after 24 h. The structure was determined by X-ray diffraction.

Formation of LPt(GMP)$_2$ (L = 5,5′-Me$_2$bipy, MepyMe$_2$t, Me$_4$dt, and Et$_4$dt and GMP = 5′- and 3′-GMP). A typical preparation of **L**Pt(GMP)$_2$ involved mixing a solution containing ∼2 equiv of GMP dissolved in 350 μL of D$_2$O at pH ∼4 and a solution containing 1 equiv (∼5 mM) of the **L**PtCl$_2$ complex in 250 μL of DMSO-d_6 to give a 1:2 ratio of Pt/GMP, and the mixture (pH ∼4) was kept at 25 °C. The mixture of D$_2$O and DMSO-d_6 solutions was employed to improve the solubility of the **L**PtCl$_2$ complex. The solution was monitored by ^{1}H NMR spectroscopy until no change in the bound versus free H8 signal intensity was observed. The **L**PtCl$_2$ complex in a D$_2$O/DMSO-d_6 mixture forms

(32) Williams, K. M.; Cerasino, L.; Intini, F. P.; Natile, G.; Marzilli, L. G. *Inorg. Chem.* **1998**, *37*, 5260–5268.
(33) Margiotta, N.; Papadia, P.; Fanizzi, F. P.; Natile, G. *Eur. J. Inorg. Chem.* **2003**, 1136–1144.
(34) Maheshwari, V.; Bhattacharyya, D.; Fronczek, F. R.; Marzilli, P. A.; Marzilli, L. G. *Inorg. Chem.* **2006**, *45*, 7182–7190.
(35) Sullivan, S. T.; Ciccarese, A.; Fanizzi, F. P.; Marzilli, L. G. *Inorg. Chem.* **2001**, *40*, 455–462.
(36) Hage, R.; Van Diemen, J. H.; Ehrlich, G.; Haasnoot, J. G.; Stufkens, D. J.; Snoeck, T. L.; Vos, J. G.; Reedijk, J. *Inorg. Chem.* **1990**, *29*, 988–993.
(37) Price, J. H.; Williamson, A. N.; Schramm, R. F.; Wayland, B. B. *Inorg. Chem.* **1972**, *11*, 1280–1284.
(38) Maheshwari, V.; Carlone, M.; Fronczek, F. R.; Marzilli, L. G. *Acta Crystallogr., Sect. B: Struct. Sci.* **2007**, *B63*, 603–611.
(39) Jensen, R. E.; Pflaum, R. T. *Anal. Chim. Acta* **1965**, *32*, 235–244.
(40) Sullivan, S. T.; Ciccarese, A.; Fanizzi, F. P.; Marzilli, L. G. *J. Am. Chem. Soc.* **2001**, *123*, 9345–9355.

a solvated complex that always remained in small amounts, along with some free GMP.

Results and Discussion

Conformational Assignments and Conformer Properties. The asymmetry of the **G** ribose residue and the local symmetry of the **L**Pt moiety influence the number of NMR signals that can be observed for each **L**Pt**G**$_2$ conformer. ^{1}H NMR spectra in the ribose region are very crowded and complex, especially for adducts with unsymmetrical carrier ligands. The downfield **G** H8 signals, in a less-crowded, more-disperse region of the spectra, are particularly useful for assessing the nature and distribution of conformers (Figure 2). Because the **G** bears a chiral ribose moiety, **L**Pt**G**$_2$ adducts with C_2-symmetrical carrier ligands (e.g., **Me$_4$dt**, **Et$_4$dt**) have one HH and two HT (ΔHT and ΛHT) NMR-distinguishable conformers (maximum total of four H8 signals), and models with unsymmetrical carrier ligands (e.g., **MepyMe$_2$t**) have two HH (HHa and HHb) and two HT (ΔHT and ΛHT) conformers (maximum total of eight H8 signals). The conformation and signal assignments of the HH atropisomers are based on the presence of nuclear Overhauser effect (NOE) cross-peaks between the two H8 signals.

At pH 6−7 for **L**Pt(GMP)$_2$ adducts, the phosphate group is deprotonated and N1 is protonated,[41,42] creating the possibility of H bonding between the phosphate group and the imino hydrogen (N1H) of the cis GMP. This interligand interaction is called "second-to-second sphere communication" (SSC) because the interacting groups are at the periphery of the cis nucleotides.[21,43,44] Such SSC interactions have been identified as important factors stabilizing the ΛHT and ΔHT conformers of the Pt adducts of 5′-GMP and 3′-GMP, respectively.[35] The CD signal shape provides a definitive means for assigning the chirality of the major HT form of **L**Pt**G**$_2$ complexes when that form clearly dominates. A CD signal shape having a positive feature at ∼290 nm and a negative feature at ∼256 nm is characteristic of the ΛHT **L**Pt**G**$_2$ conformer,[21,31,32,43,45] whereas a CD signal shape having a negative feature at ∼290 nm and a positive feature at ∼256 nm is characteristic of the ΔHT conformer of **L**Pt**G**$_2$ adducts.[31,32,43,46] The CD signal of HH conformers is generally weak, a feature attributable to the inherent symmetry of the base chromophore, with the two bases having a pseudo mirror relationship in HH conformers.

H8 Shifts and Base Canting. In addition to the HH or HT **G** base orientation, **G** base canting is another significant structural parameter of **L**Pt**G**$_2$ conformers. A given base is generally not oriented with its plane exactly perpendicular to the coordination plane, but it is canted. The canting can be either left-handed (L) or right-handed (R) (Figure 3). Useful indications for assessing the degree of **G** base canting are provided by the **G** H8 signal shifts.[14] The H8 shift is influenced by the positioning of the H8 atom with respect to the shielding cone of the cis **G** base. In a HT arrangement, the canting may move the six-membered rings either closer to the midpoint between the N7 atoms ("6-in" form) or farther from this midpoint ("6-out" form). The canting of the bases in the direction ("6-out" form) that moves each H8 toward the cis **G** will lead to greater H8 shielding and, hence, an upfield H8 signal relative to the average H8 signal. The minor HT conformer typically is "6-out". In contrast, the canting of the base that moves its H8 away from the cis **G** will lead to less H8 shielding or perhaps deshielding in the HT form[26] and thus a more downfield H8 signal. The major HT conformer typically is "6-in".

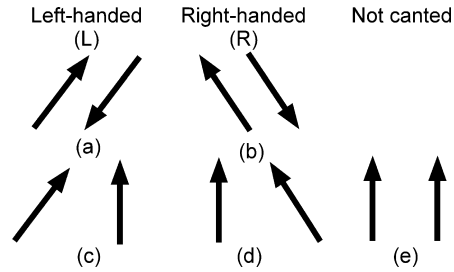

Figure 3. Shorthand representation for left-handed (L; a, c) and right-handed (R; b, d) canting for **L**Pt**G**$_2$ adducts. In the ΔHT conformer shown (a, b), L and R canting have the six-membered ring far from the C_2 axis for L canting ("6-out") and close to the axis for R canting ("6-in"). For the ΛHT conformer (not shown), the arrows are all rotated by 180°. The HH conformer can be left-handed (c), right-handed (d), or not canted (e).

For the HH orientation, one base is typically more canted, with its H8 toward the other cis base, which is less canted.[19,30,31] The H8 atom of the more canted **G** is closest to the shielding region of the cis **G** and has a relatively upfield H8 signal (HH_u). The H8 signal of the less canted base is relatively downfield (HH_d) because this H8 is farthest from the cis **G** base shielding region and may be in the deshielding region of this base.[31,44] Typically, the HH_u and HH_d H8 signals are separated by ∼1 ppm and straddle the HT H8 signals. In less common cases, the HH bases are not canted and the two signals are relatively downfield.

(5,5′-Me$_2$bipy)Pt(5′-GMP)$_2$. Four new H8 signals of the (**5,5′-Me$_2$bipy**)Pt(5′-GMP)$_2$ adduct downfield from the free 5′-GMP H8 signal at 8.22 ppm were observed at 25 °C (Figure 4). When the pH was raised from 4.0 to 7.5, the H8 signal at 8.81 ppm shifted slightly upfield by 0.02 ppm and became the most dominant signal. The CD signal shape observed for this adduct at pH 7.5 is characteristic of the ΛHT conformer (Figure 5). For the 5′-GMP adducts, the ΛHT conformer is more favored by SSC upon phosphate deprotonation;[16] therefore, the dominant H8 signal of the (**5,5′-Me$_2$bipy**)Pt(5′-GMP)$_2$ adduct was assigned to the ΛHT conformer. The intensity of the H8 signals at 9.11 and 9.01 ppm (pH 4.0) remained comparable throughout the pH titration. These H8 signals shifted downfield by ∼0.11−0.14 ppm when the pH was increased to 7.5. The two H8 signals were connected through a NOE cross-peak in a ROESY spectrum collected at 5 °C and were thus assigned to the

(41) Sigel, H.; Lippert, B. *Pure Appl. Chem.* **1998**, *70*, 845.
(42) Sigel, H.; Massoud, S. S.; Corfu, N. A. *J. Am. Chem. Soc.* **1994**, *116*, 2958–2971.
(43) Wong, H. C.; Shinozuka, K.; Natile, G.; Marzilli, L. G. *Inorg. Chim. Acta* **2000**, *297*, 36–46.
(44) Saad, J. S.; Scarcia, T.; Shinozuka, K.; Natile, G.; Marzilli, L. G. *Inorg. Chem.* **2002**, *41*, 546–557.
(45) Wong, H. C.; Coogan, R.; Intini, F. P.; Natile, G.; Marzilli, L. G. *Inorg. Chem.* **1999**, *38*, 777–787.
(46) Wong, H. C.; Intini, F. P.; Natile, G.; Marzilli, L. G. *Inorg. Chem.* **1999**, *38*, 1006–1014.

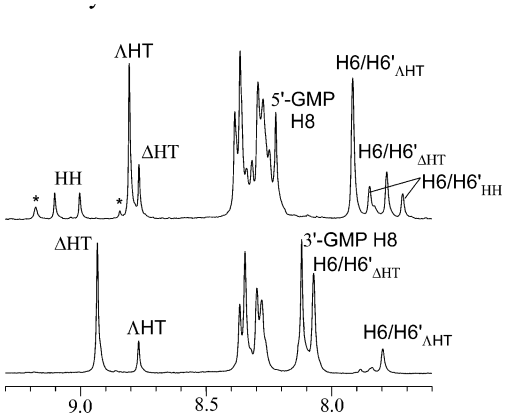

Figure 4. Aromatic region of ^{1}H NMR spectra of (**5,5′-Me$_2$bipy**)Pt(5′-GMP)$_2$ (top) and (**5,5′-Me$_2$bipy**)Pt(3′-GMP)$_2$ (bottom) at pH ∼ 4.0 and 25 °C. The H8 signals for the conformers are designated by the conformation. (Pyridyl H6′ signals attributed to the solvated Pt complex are indicated by asterisks).

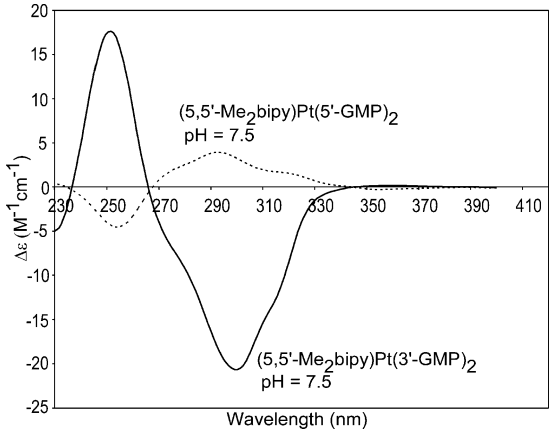

Figure 5. CD spectra of (**5,5′-Me$_2$bipy**)Pt(5′-GMP)$_2$ and (**5,5′-Me$_2$bipy**)Pt(3′-GMP)$_2$ at 25 °C.

Table 1. Chemical Shifts (ppm) of the H8 Signals of **L**Pt(GMP)$_2$ Adducts (**L** = **5,5′-Me$_2$bipy**, **Et$_4$dt**, **Me$_4$dt**) at 5 °C[a]

complex	pH	ΔHT	ΛHT	HH_d	HH_u
(**5,5′-Me$_2$bipy**)Pt(5′-GMP)$_2$[b]	4.0	8.77	8.81	9.11	9.01
	7.5	8.72	8.79	9.25	9.12
(**5,5′-Me$_2$bipy**)Pt(3′-GMP)$_2$[b]	4.0	8.88	8.76	*c*	*c*
	7.5	8.87	8.75	*c*	*c*
(**Et$_4$dt**)Pt(5′-GMP)$_2$	4.0	9.06	8.96	9.18	8.83
	7.5	9.04	8.99	9.37	8.96
(**Et$_4$dt**)Pt(3′-GMP)$_2$	4.0	9.01	8.87	*c*	*c*
	7.5	9.01	8.88	*c*	*c*
(**Me$_4$dt**)Pt(5′-GMP)$_2$	4.0	9.08	8.96	9.10	8.66
	7.0	9.06	8.95	9.27	8.74
(**Me$_4$dt**)Pt(3′-GMP)$_2$	4.0	8.85	8.83	*c*	*c*
	7.0	8.89	8.92	*c*	*c*

[a] Subscripted letters d and u are used to distinguish the downfield and the upfield H8 signals, respectively, for a given conformer. Signal assignments are based on the 2D NMR and pH titration studies. [b] NMR spectrum recorded at 25 °C. [c] Signal not detected.

HH conformer. The signal at 8.77 ppm was assigned to the ΔHT conformer, the only remaining possible conformer. The H8 chemical shifts at pH 4.0 and 7.5 are listed in Table 1. From pH 4.0 to 7.5, the distribution of the ΛHT, ΔHT, and HH conformers changed from 42%, 29%, and 29% to 58%, 23%, and 18%, respectively.

The H8 signals of the HH conformer of the (**5,5′-Me$_2$bipy**)Pt(5′-GMP)$_2$ adduct have low dispersion (0.10 ppm), and both are relatively downfield when compared to the HT H8 signals. A similar unusual H8 shift pattern was reported for the HH conformer of the (**Me$_2$ppz**)Pt(5′-GMP)$_2$ adduct (**Me$_2$ppz** = *N*,*N*′-dimethylpiperazine) and was attributed to a low degree of base canting.[21] The H8 signals of the (**5,5′-Me$_2$bipy**)Pt(5′-GMP)$_2$ HH conformer have a downfield shift because the two bases have relatively little canting, and as a result, H8 experiences less shielding by the cis **G** and possibly greater deshielding by the anisotropic Pt atom.[35,47−49] For the (**5,5′-Me$_2$bipy**)Pt(5′-GMP)$_2$ adduct, the H8 signal of the major ΛHT conformer is downfield to that of the minor ΔHT conformer. In typical cases for the HT conformers, the "6-in" form is favored.[20,50] The H8 signal of the "6-in" form is downfield because the H8 atoms are positioned away from the cis base, while the H8 signal of the "6-out" form is upfield because the H8 signals of the two bases are shielded by the cis base. For the (**5,5′-Me$_2$bipy**)Pt(5′-GMP)$_2$ adduct, the major ΛHT conformer is the "6-in" form, thus L-canted, and the minor ΔHT conformer is the "6-out" form with L canting (Figure 3).

The absence of H8−H8 exchange spectroscopy (EXSY) cross-peaks in the ROESY spectrum of (**5,5′-Me$_2$bipy**)Pt(5′-GMP)$_2$ indicates that interconversion between the rotamers is slow. Rotation is probably impeded by the steric effect of the pyridyl H6/H6′ atoms of **5,5′-Me$_2$bipy**, which are the pyridyl ring atoms closest to the cis 5′-GMPs, as evident from models and from the observation of H8−H6/H6′ NOE cross-peaks. During rotation, the **G** O6 clashes with the pyridyl ring C6H. A further indication of this proximity is the finding that the pyridyl H6/H6′ signals of the (**5,5′-Me$_2$bipy**)Pt(5′-GMP)$_2$ adduct are shifted upfield by 1.0−1.4 ppm, when compared to the H6/H6′ signals (9.19 and 8.81 ppm) of the solvated Pt precursor. The anisotropy of the cis-coordinated **G** base is responsible for these large upfield shifts. A similar upfield shift was observed for the H6/H6′ signal of the [(**MepyMe$_2$t**)Pt(Guo)$_2$]$^{2+}$ adduct[34] and for the signals of the similarly positioned phenanthroline (**phen**) protons in the [(**phen**)Pt(Guo)$_2$]$^{2+}$ adduct.[33]

(5,5′-Me$_2$bipy)Pt(3′-GMP)$_2$. Two H8 signals downfield from the free 3′-GMP H8 signal at 8.11 ppm were observed at 25 °C and were assigned to the HT conformers of the (**5,5′-Me$_2$bipy**)Pt(3′-GMP)$_2$ adduct (Table 1 and Figure 4). From pH 4.0 to 7.5, the intensity of the H8 signal at 8.88 ppm increased, while that for the H8 signal at 8.76 ppm decreased. The CD signal shape at pH 7.5 was characteristic of the ΔHT conformer (Figure 5). For the 3′-GMP adducts, the ΔHT conformer is known to be stabilized by SSC upon phosphate deprotonation (pH ∼7.0).[19,32,35,46] Therefore, this major H8 signal was assigned to the ΔHT conformer. The H8 signal at 8.76 ppm was assigned to the ΛHT conformer. From pH 4.0 to 7.5, the conformation distribution of the ΔHT and ΛHT conformers changed from 73% and 27% to 80% and 20%, respectively. The H8 signal of the major ΔHT

(47) Carlone, M.; Fanizzi, F. P.; Intini, F. P.; Margiotta, N.; Marzilli, L. G.; Natile, G. *Inorg. Chem.* **2000**, *39*, 634–641.
(48) Elizondo-Riojas, M.-A.; Kozelka, J. *Inorg. Chim. Acta* **2000**, *297*, 417–420.
(49) Sundquist, W. I.; Lippard, S. J. *Coord. Chem. Rev.* **1990**, *100*, 293–322.
(50) Natile, G.; Marzilli, L. G. *Coord. Chem. Rev.* **2006**, *250*, 1315–1331.

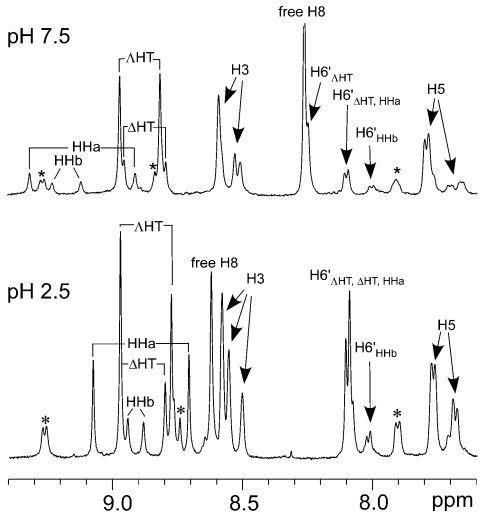

Figure 6. Aromatic region of ^{1}H NMR spectra of (**MepyMe$_2$t**)Pt(5′-GMP)$_2$ at pH 2.5 (bottom) and pH 7.5 (top) at 25 °C. The H8 signals for the conformers are designated by the conformation. (Pyridyl signals attributed to the solvated Pt complex are indicated by asterisks).

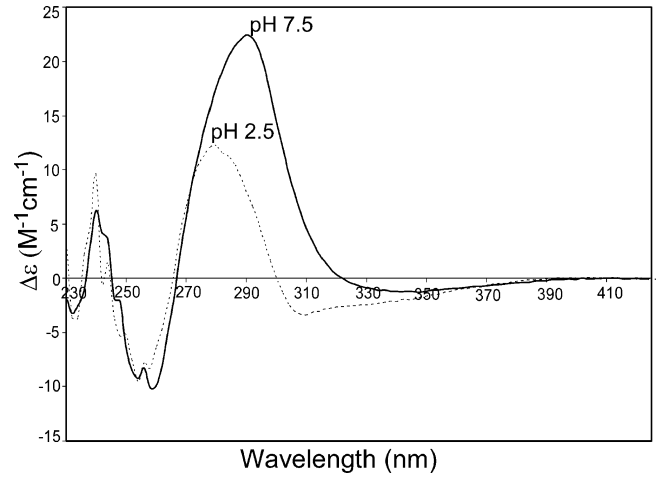

Figure 7. CD spectra of (**MepyMe$_2$t**)Pt(5′-GMP)$_2$ at pH 2.5 and pH 7.5 at 25 °C.

Table 2. Chemical Shifts (ppm) of the H8 Signals of (**MepyMe$_2$t**)Pt(GMP)$_2$ Adducts at 25 °C[a]

		ΔHT		ΛHT		HHa		HHb	
complex	pH	ΔHT_d (py)	ΔHT_u (t)	ΛHT_d (py)	ΛHT_u (t)	HHa_d (t)	HHa_u (py)	HHb_d (t)	HHb_u (py)
(**MepyMe$_2$t**)-Pt(5′-GMP)$_2$	2.5	8.96	8.83	8.96	8.78	9.08	8.71	8.94	8.88
	7.5	8.96_2	8.81_4	8.95_8	8.80_7	9.31	8.91	9.23	9.10
(**MepyMe$_2$t**)-Pt(3′-GMP)$_2$	4.5	8.95	8.84	8.89	8.74	*b*		*b*	
	7.5	8.89	8.81	8.89	8.74	*b*		*b*	

[a] The py and t notations designate **G**'s cis to the pyridyl and triazine rings, respectively. Subscripted letters d and u are used for downfield and upfield H8 signals, respectively, for a given conformer. Third decimal place subscripted numbers are used to distinguish signals with very similar chemical shifts. Signal assignments are based on the 2D NMR and pH titration studies. [b] Signal not detected.

conformer is 0.17 ppm downfield from that of the minor ΛHT conformer. From this relationship, the "6-in" major form is ΔHT R, and the "6-out" minor form is ΛHT R (cf. Figure 3). Neither NOE nor EXSY cross-peaks were observed between the H8 signals of the (**5,5′-Me$_2$bipy**)Pt(3′-GMP)$_2$ adduct. Strong H8−H6/H6′ NOE cross-peaks at 8.06 and 8.88 ppm for the ΔHT conformer and at 7.79 and 8.76 ppm were observed for the ΛHT conformer. Of particular note, the HH conformer was not detected for this adduct, even at 5 °C, thus reinforcing the general finding that the 5′-phosphate group stabilizes the HH conformer more than the 3′-phosphate group does.[35,44] When conformer interchange is slow, the HH conformer is usually found for **L**Pt(3′-GMP)$_2$ adducts. For example, at pH 3.3 for the (**Me$_2$ppz**)Pt(GMP)$_2$ adducts, the amount of HH conformer observed for the 3′-GMP adduct was small (∼8%), in comparison to ∼24% HH conformer for the 5′-GMP adduct.[21] The (**5,5′-Me$_2$bipy**)Pt(3′-GMP)$_2$ adduct, in fact, presents the first case in which no HH conformer is found for a 3′-GMP adduct with slowly interchanging rotamers.

(MepyMe$_2$t)Pt(5′-GMP)$_2$. Within 2 h of mixing (**MepyMe$_2$t**)PtCl$_2$ with 5′-GMP in a 1:2 molar ratio at pH ∼4.0 at 25 °C, four pairs of new H8 signals downfield from the free 5′-GMP H8 signal were present. As the pH was varied from 2.5 to 7.5, the H8 signals at 8.96 and 8.78 ppm became the most dominant signals (Figure 6). A CD signal shape characteristic of the ΛHT conformer was observed for (**MepyMe$_2$t**)Pt(5′-GMP)$_2$ at pH 7.5 and below (Figure 7). The CD signal intensity was stronger at pH 7.5 than at pH 2.5, consistent with the higher stability of the ΛHT conformer caused on phosphate deprotonation resulting from SSC.[21,43,44] Thus, the larger H8 signals (at 8.96 and 8.78 ppm at pH 2.5) were assigned to the ΛHT conformer.

In a ROESY spectrum of the (**MepyMe$_2$t**)Pt(5′-GMP)$_2$ adduct at pH 2.5 (where the H8 signals of this adduct were most widely dispersed), a weak NOE cross-peak present between the two comparably sized H8 signals at 9.08 and 8.71 ppm establishes the HH conformation (Table 2 and

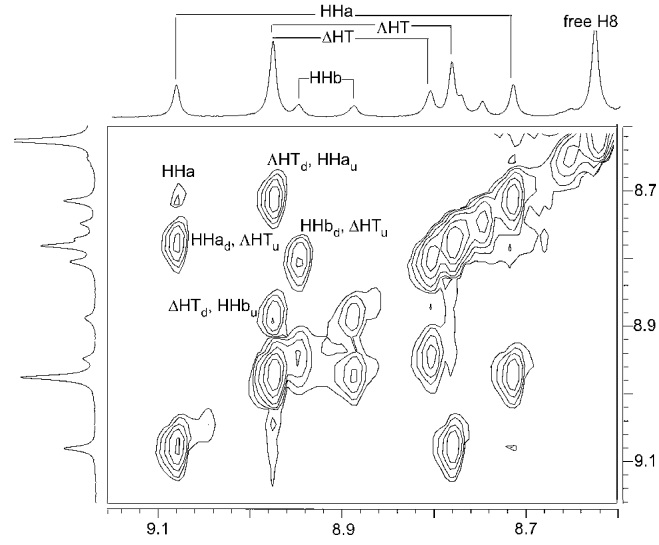

Figure 8. ROESY spectrum of the (**MepyMe$_2$t**)Pt(5′-GMP)$_2$ adduct in the aromatic region at pH 2.5 and 25 °C. The cross-peak labeled as HHa is a NOE between the two H8 signals of the HHa conformer. The other labeled cross-peaks are EXSY peaks between the H8 signals of two different conformers.

Figure 8). This HH conformer (assigned as HHa, see below) is the second most abundant conformer of the (**MepyMe$_2$t**)-Pt(5′-GMP)$_2$ adduct. These two HH H8 signals are well-

dispersed and straddle the signals of the HT conformers, the usual H8 chemical shift pattern.[19,30,31] The remaining two pairs of H8 signals must belong to the ΔHT and HHb conformers. However, because of the unusual properties of these conformers and the unsymmetrical nature of the carrier ligand, we turned to a pH study to make the assignment of conformation.

From pH 2.5 to pH 7.5, the H8 signals for the (**MepyMe$_2$t**)-Pt(5′-GMP)$_2$ HHa rotamer shifted significantly downfield by 0.23 and 0.20 ppm (Figure 6). Typically, a ca. 0.2 ppm downfield shift was observed for HH rotamers[20,21] upon phosphate deprotonation; this effect may be explained by the "wrong-way shift" attributed to the higher deshielding effect of the deprotonated phosphate group as it is positioned in the HH conformer.[20,51] However, the H8 signals of the HT conformers do not shift significantly in the pH ∼2−7 range.[21,35,44] Consistent with this pattern, the H8 signals of the (**MepyMe$_2$t**)Pt(5′-GMP)$_2$ ΛHT conformer shifted very little (Table 2, Figure 6), whereas a ca. 0.2 ppm downfield shift occurred for the H8 signal of the HH conformer of the (**R$_4$dt**)Pt(5′-GMP)$_2$ adducts discussed below.

One of the two pairs of H8 signals of the (**MepyMe$_2$t**)Pt(5′-GMP)$_2$ adduct (at 8.94 and 8.88 ppm) not assigned above shifted downfield by more than 0.2 ppm from pH 2.5 to 7.5 (Table 2, Figure 6); this pair is assigned to HHb. However, because of the low abundance of the HHb conformer, no H8-to-H8 NOE cross-peak was observed in the ROESY spectrum for the (**MepyMe$_2$t**)Pt(5′-GMP)$_2$ adduct. The remaining pair of H8 signals shifted only slightly upfield from pH 2.5 to 7.5 (Table 2, Figure 6), consistent with an assignment to the only other possible conformer, ΔHT.

For the (**MepyMe$_2$t**)Pt(5′-GMP)$_2$ adduct, the H8 to pyridyl H6′ NOE cross-peaks can be used to determine which H8 signal belongs to the 5′-GMP cis to the pyridyl ring and by default which H8 signal belongs to the 5′-GMP cis to the triazine ring. Because the ΔHT and ΛHT conformers are assigned, the orientation of the **G** bases relative to these ligand rings is established for the HT conformers. The pyridyl H6′ signals of the (**MepyMe$_2$t**)Pt(5′-GMP)$_2$ adduct (overlapping at 8.0−8.1 ppm) have NOE cross-peaks to the downfield H8 signals of the ΛHT and ΔHT conformers (overlapping at 8.96 ppm) and to the upfield H8 signals of the HHa conformer (at 8.71 ppm) and the HHb conformer (at 8.88 ppm). These H8 signals are assigned to the 5′-GMP cis to the pyridyl ring.

As can be seen from Figure 2, where N′ represents the pyridyl ring, the base next to this ring has an orientation with respect to the coordination plane that is the same in the ΛHT and HHa pair. Likewise, the orientation of this base is the same in the ΔHT and HHb pair. The rotation of the 5′-GMP cis to the pyridyl ring is expected to be slow; thus, conformer interchange involving such rotation will be too slow to generate detectable EXSY cross-peaks. (Slow interconversion between rotamers is depicted by short arrows in this figure.) Each HT conformer can exchange rapidly (depicted by long arrows) with only one HH conformer because only the base cis to the triazine ring can rotate rapidly. For example, the H8 signal of the **G** in the ΔHT rotamer cis to the triazine ring at 8.83 ppm has an EXSY cross-peak with the downfield H8 signal of the HHb rotamer at 8.94 ppm; this H8 signal of the HHb rotamer belongs to the 5′-GMP cis to the triazine ring. Such EXSY cross-peaks between the H8 signals of the 5′-GMP cis to the triazine ring of the HH and HT rotamers were used for the unambiguous assignment of the HH conformers as HHa and HHb because the ΔHT and the ΛHT H8 signals of the 5′-GMP cis to the pyridyl ring overlap at 8.96 ppm.

We apply the foregoing reasoning to all four H8−H8 EXSY cross-peaks in the ROESY spectrum of the (**MepyMe$_2$t**)Pt(5′-GMP)$_2$ adduct at 25 °C (Figure 8). The EXSY cross-peaks observed are between the H8 signals of the HHa and the ΛHT rotamers (9.08 and 8.78 ppm (cis to the triazine ring) and 8.71 and 8.96 ppm (cis to the pyridyl ring)) and between the H8 signals of the HHb and the ΔHT rotamers (8.94 and 8.83 ppm (cis to the triazine ring) and 8.88 and 8.96 ppm (cis to the pyridyl ring)).

For the (**MepyMe$_2$t**)Pt(5′-GMP)$_2$ adduct, as the pH was increased from 2.5 to 7.5, the population of the ΛHT, HHa, ΔHT, and HHb conformers changed from 40%, 30%, 20%, and 10% to 65%, 10%, 20%, and 5%, respectively (Figure 6). For this adduct, the combined abundance of the HT conformers is greater than the combined abundance of the HH conformers, a typical situation.[50] It is also typical for the percentage of the HH conformers to decrease with increasing pH.[20]

At pH 7.5 and below, the HHa conformer of (**MepyMe$_2$t**)-Pt(5′-GMP)$_2$ is more abundant and has more H8-to-H8 signal dispersion (0.37 ppm) than the HHb conformer (0.06 ppm). For HHa, the 5′-GMP cis to the pyridyl ring has the upfield shift, so the base is canted with its H8 atom projecting toward the shielding region of the 5′-GMP cis to the triazine ring. This 5′-GMP is either not canted or only slightly canted. Canting in the HHa conformer (Figure 2, where N′ represents the pyridyl ring) is right-handed (R). However, the small H8 signal dispersion for the HHb conformer of the (**MepyMe$_2$t**)Pt(5′-GMP)$_2$ adduct is associated with a low degree of canting,[21,22] similar to that observed for the (**5,5′-Me$_2$bipy**)-Pt(5′-GMP)$_2$ adduct. The orientation of the two 5′-GMP bases in HHb may be nearly perpendicular to the Pt coordination plane or may be slightly canted. Alternatively, the two bases may be "wagging", rapidly changing the canting direction between the R- and L-canted orientations, leading to shift averaging and thereby accounting for the small HH H8 signal dispersion.

(MepyMe$_2$t)Pt(3′-GMP)$_2$. Qualitatively, for **G** derivatives, the rate of rotation about the Pt−N7 bond increases in the order 5′-GMP < 3′-GMP < Guo < 9-Et**G** (9-Et**G** = 9-ethylguanine).[19,31,32,47,52] Previously, we observed only four H8 signals for (**MepyMe$_2$t**)Pt(Guo)$_2$.[34] We attributed this finding to fast interchange within each of the pairs (ΛHT/HHa and ΔHT/HHb), a process involving **G** base rotation for the Guo cis to the triazine ring (Figure 2). Also, rotation

(51) Martin, R. B. *Acc. Chem. Res.* **1985**, *18*, 32–38.

(52) Colonna, G.; Di Masi, N. G.; Marzilli, L. G.; Natile, G. *Inorg. Chem.* **2003**, *42*, 997–1005.

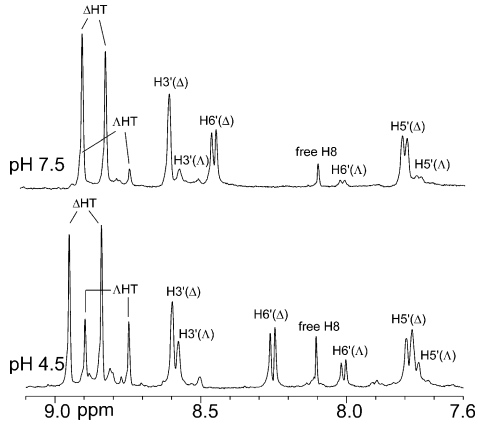

Figure 9. Aromatic region of ^{1}H NMR spectra of (**MepyMe$_2$t**)Pt(3′-GMP)$_2$ at pH 4.5 (bottom) and pH 7.5 (top) at 25 °C. The H8 signals for the conformers are designated by the conformation.

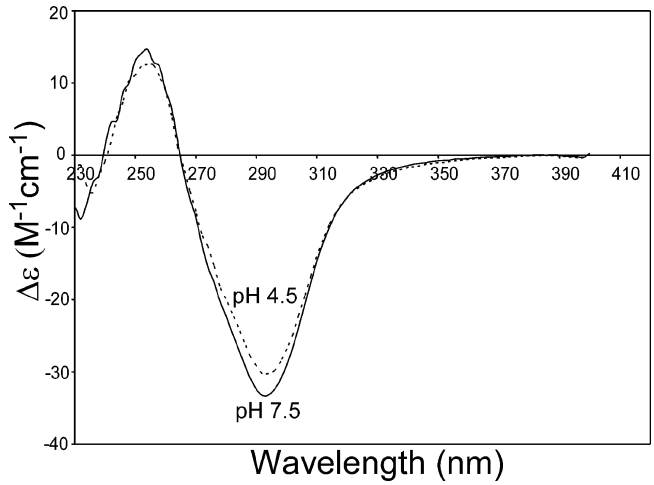

Figure 10. CD spectra of (**MepyMe$_2$t**)Pt(3′-GMP)$_2$ at pH 4.5 and 7.5 at 25 °C.

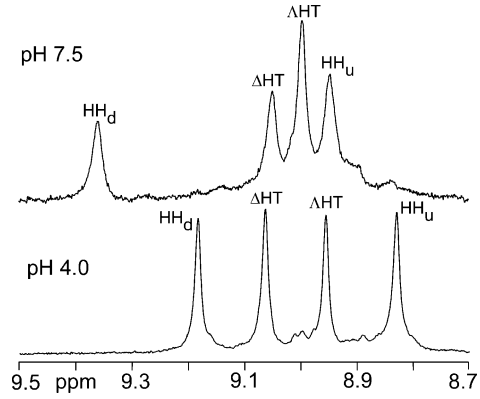

Figure 11. H8 region of the ^{1}H NMR spectra of (**Et$_4$dt**)Pt(5′-GMP)$_2$ at 5 °C.

of the Guo cis to the pyridyl group was postulated to be a slow process, as now confirmed for the (**MepyMe$_2$t**)Pt(5′-GMP)$_2$ adduct, which exhibited no interchange (no EXSY peaks) between the two pairs.

Two pairs of H8 signals in a 2:1 ratio were observed for the (**MepyMe$_2$t**)Pt(3′-GMP)$_2$ adduct at pH 4.5 and 25 °C (Figure 9). Neither NOE nor EXSY cross-peaks were observed between these H8 signals; a NOE cross-peak is expected for a HH conformer. Therefore, even for a rapid HT/HH equilibrium, a NOE cross-peak would be found if either HT/HH pair had a significant amount of the HH conformer. The H8 NMR signals of the HH conformer were not detectable even at a low temperature (0 °C), a result similar to that found for the (**pipen**)Pt(3′-GMP)$_2$[46] (**pipen** = 2-aminomethylpiperidine) and [(**MepyMe$_2$t**)Pt(Guo)$_2$]$^{2+}$ adducts. Thus, the H8 signals of the (**MepyMe$_2$t**)Pt(3′-GMP)$_2$ adduct arising from two sets of rapidly interchanging pairs of conformers, ΔHT/HHa and ΛHT/HHb, reflect primarily a dominant HT conformer, as discussed previously.[34] The two pairs of HT and HH conformers interchange within the pair but not between pairs. The four H8 signals for the (**MepyMe$_2$t**)Pt(3′-GMP)$_2$ adduct thus reflect mainly the two HT conformers, ΔHT and ΛHT. From the order of rotation rates for the various **G** derivatives, it was uncertain what pattern of behavior to expect, but now it is clear that (**MepyMe$_2$t**)Pt(3′-GMP)$_2$ has dynamic properties more similar to those of (**MepyMe$_2$t**)Pt(Guo)$_2$ than to those of (**MepyMe$_2$t**)Pt(5′-GMP)$_2$.

From 4.5 to 7.5, the more downfield of the two H8 signals of the major HT rotamer of (**MepyMe$_2$t**)Pt(3′-GMP)$_2$ (at 8.95 ppm) shifted slightly upfield, overlapping with the downfield H8 signal of the minor HT rotamer at 8.89 ppm (Table 2). The other H8 signals showed no significant shift until pH 7.5. As the pH was increased from 4.5 to 7.5, the major HT rotamer became the almost exclusively observed atropisomer (Figure 9). The CD spectra collected at pH 4.5 and 7.5 are characteristic of the ΔHT conformer (Figure 10). Therefore, at pH 4.5, the H8 signals at 8.95 and 8.84 ppm belonging to the major HT conformer are assigned to the ΔHT conformer stabilized by SSC, while the H8 signals at 8.89 and 8.74 ppm are assigned to the ΛHT conformer (minor). This previously reported downfield relationship of the H8 signal of the major HT conformer to the respective H8 signal of the minor HT conformer[19,23,30,31,44] is consistent with the major ΔHT conformer being "6-in" (R canting) and the minor ΛHT conformer being "6-out" (L canting).

The properties of the (**MepyMe$_2$t**)Pt(3′-GMP)$_2$ adduct at pH 4.5 were explored further in ROESY studies. From the NOE cross-peaks, the H8 signals belonging to the 3′-GMP cis to the pyridyl ring of the HT conformers of the (**MepyMe$_2$t**)Pt(5′-GMP)$_2$ adduct were also downfield compared to those of the 3′-GMP cis to the triazine ring. For the (**MepyMe$_2$t**)Pt(3′-GMP)$_2$ adduct, the H6′ doublets of the ΔHT and ΛHT conformers (Figure 9 and Supporting Information) were shifted upfield by 1.01 and 1.24 ppm from the H6′ signal of the solvated Pt complex at 9.26 ppm; similar behavior was observed for the H6′ signal of the (**5,5′-Me$_2$bipy**)Pt(3′-GMP)$_2$ adduct. These large H6′ upfield shifts can be attributed to the anisotropic effect of the cis-coordinated base but cannot easily be correlated with the degree of canting.

(Et$_4$dt)Pt(5′-GMP)$_2$. Four new H8 signals of comparable intensities were observed within 24 h of mixing 1 equiv of (**Et$_4$dt**)PtCl$_2$ with 2 equiv of 5′-GMP at 25 °C (Figure 11). Sharp ^{1}H NMR signals were observed at 25 °C for the (**Et$_4$dt**)Pt(5′-GMP)$_2$ adduct at pH ∼4; however, in order to compare the data with the (**Me$_4$dt**)Pt(5′-GMP)$_2$ adduct (Supporting Information), 1D ^{1}H NMR spectra and a ROESY

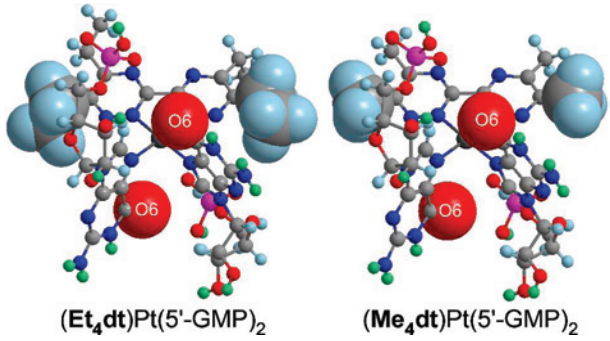

Figure 12. Greater steric clashes between substituents at the 6,6′ position of the **R₄dt** carrier ligand and the **G** O6 for the **Et₄dt** adduct compared to the **Me₄dt** adduct.

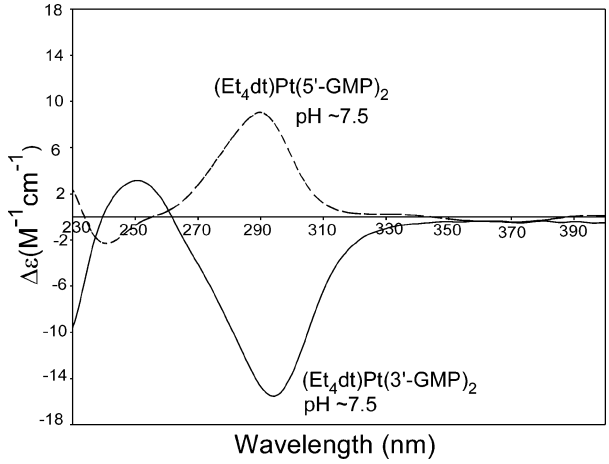

Figure 13. CD spectra of (**Et₄dt**)Pt(5′-GMP)$_2$ and (**Et₄dt**)Pt(3′-GMP)$_2$ at 25 °C.

spectrum were collected at 5 °C. At 25 °C, the full width at half-maximum (fwhm) of the H8 signals for (**Et₄dt**)Pt(5′-GMP)$_2$ was 6 Hz for all three rotamers, as compared to the fwhm of the H8 signals of (**Me₄dt**)Pt(5′-GMP)$_2$ of 11 (ΔHT), 10 (ΛHT), 12 (HH$_d$), and 11 (HH$_u$) Hz. These H8 signals of the (**Et₄dt**)Pt(5′-GMP)$_2$ adduct at 25 °C were even sharper than those of the (**Me₄dt**)Pt(5′-GMP)$_2$ adduct at 5 °C, where all fwhm values were ∼7 Hz. These comparisons clearly indicate that the rotation rate about the Pt−N7 bond is considerably slower for (**Et₄dt**)Pt(5′-GMP)$_2$ than for (**Me₄dt**)-Pt(5′-GMP)$_2$, probably because of steric clashes between the 5′-GMP O6 and the methyl group of the 6,6′ ethyl groups of the **Et₄dt** ligand in the (**Et₄dt**)Pt(5′-GMP)$_2$ adduct as the **G** base rotates (Figure 12).

When the pH of solutions containing (**Et₄dt**)Pt(GMP)$_2$ adducts was raised from ∼4 to 7.5 (above pH 7.5, the adduct decomposed, as evidenced by an increase in the intensity of the free GMP H8 signal), the H8 signal at 8.96 ppm shifted slightly downfield to 8.99 ppm and became the most dominant signal (Figure 11); this peak was assigned to the ΛHT conformer because the CD signal shape observed for this solution is characteristic of the ΛHT conformation (Figure 13).[31,32,35,45,46] SSC interactions stabilize the ΛHT conformer of **L**Pt(5′-GMP)$_2$ adducts at or near neutral pH.[35,43,44] At pH 4.0, a NOE cross-peak was observed between the two dispersed, comparably sized H8 signals at 9.18 and 8.83 ppm (Figure 14). These characteristics allow

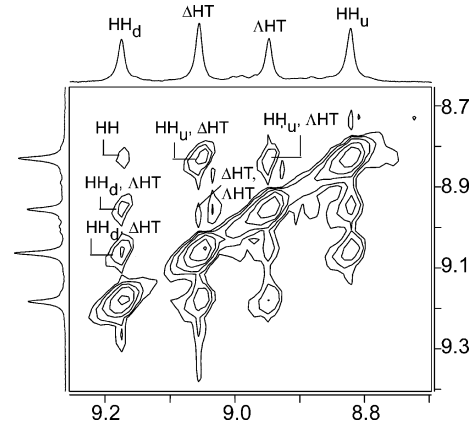

Figure 14. H8 region of the ROESY spectrum of (**Et₄dt**)Pt(5′-GMP)$_2$ at pH 4.0 and 5 °C. The cross-peak labeled as HH is a NOE between the H8 signals of a HH conformer. The other labeled cross-peaks are EXSY peaks between the H8 signals of different rotamers.

unambiguous assignment of these H8 signals to the HH rotamer. The H8 signals of the HH rotamer for the (**Et₄dt**)-Pt(5′-GMP)$_2$ adduct at both high and low pH values were ∼0.08−0.22 ppm more downfield than those for the (**Me₄dt**)-Pt(5′-GMP)$_2$ adduct (Table 1). The remaining H8 signal of the (**Et₄dt**)Pt(5′-GMP)$_2$ adduct at 9.06 ppm (pH 4.0) was assigned to the ΔHT rotamer. From pH 4.0−7.5, no significant shift was observed for the H8 signals of the HT rotamers; however, the HH$_d$ and the HH$_u$ signals shifted downfield by 0.19 and 0.13 ppm, respectively.

In contrast to the typical H8 chemical shift pattern of the major and the minor HT conformers,[19,23,30,31,44] the H8 signal of the major HT conformer (ΛHT) of the (**Et₄dt**)Pt(5′-GMP)$_2$ adduct (at pH 7.5) is upfield from that of the minor HT conformer (ΔHT). Because the H8 signals of the HT conformers are relatively more downfield and the difference in the chemical shifts is small (0.10 ppm), it is not clear if this unusual HT H8 signal shift pattern is because of a relatively more upfield ΛHT H8 signal or a more downfield ΔHT H8 signal. The H8 signals of the HT conformers of the (**Et₄dt**)Pt(5′-GMP)$_2$ adduct are positioned between the two H8 signals of the HH conformer. Thus, the H8 shifts of the HT conformers are not particularly unusual. Because of the symmetrical nature of the carrier ligand in (**Et₄dt**)Pt(5′-GMP)$_2$, the bases in HT conformers may "wag" between R and L canting, causing the H8 signals of the conformers to have similar shifts. The H8 chemical shift pattern (separation of 0.35 ppm) for the HH conformer of (**Et₄dt**)Pt(5′-GMP)$_2$ is similar to that of the HH conformer of (**MepyMe₂t**)Pt(5′-GMP)$_2$. The moderately large H8 signal dispersion (0.35 ppm) for the (**Et₄dt**)Pt(5′-GMP)$_2$ HH conformer is attributable to different canting of the two bases.

Five EXSY cross-peaks were observed in a ROESY spectrum of (**Et₄dt**)Pt(5′-GMP)$_2$, collected at 5 °C (Figure 14). The two H8 signals of the HH rotamer have cross-peaks with the H8 signals of both the ΛHT and ΔHT rotamers. Also, a weak EXSY cross-peak was observed between the H8 signals of the ΛHT and the ΔHT rotamers. Because both 5′-GMPs are cis to the sterically less-impeding triazine rings, Pt−N7 rotation is fast enough for the H8 signals of the rotamers to have EXSY cross-peaks. In contrast, interchange

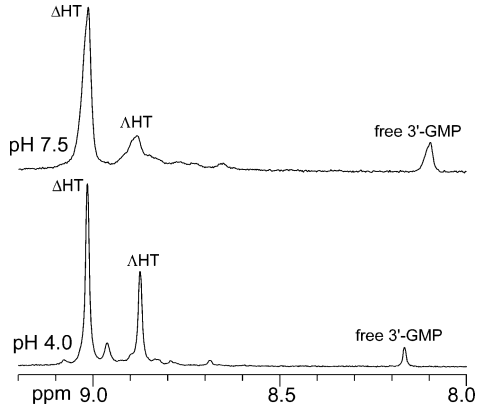

Figure 15. H8 region of the ^{1}H NMR spectra of (**Et$_4$dt**)Pt(3′-GMP)$_2$ at 5 °C.

between rotamers is slower in ligands containing a pyridyl moiety, as evidenced by the absence of any H8−H8 EXSY cross-peaks for (**5,5′-Me$_2$bipy**)Pt(5′-GMP)$_2$. In addition, H8−H8 cross-peaks between the ΛHT and the ΔHT conformers were absent for the (**MepyMe$_2$t**)Pt(5′-GMP)$_2$ adduct. The broad NMR signals observed at 25 °C for the (**Me$_4$dt**)Pt(5′-GMP)$_2$ adduct can be attributed to exchange between conformers and provide further evidence for facile interchange between rotamers in the (**R$_4$dt**)Pt(5′-GMP)$_2$ adducts.

For the (**Et$_4$dt**)Pt(5′-GMP)$_2$ adduct, increasing the pH from 4.0 to 7.5 changed the distribution of the HH, ΛHT, and ΔHT rotamers from 50%, 25%, and 25% to 40%, 37%, and 23%, respectively (Figure 11). For both (**Et$_4$dt**)Pt(5′-GMP)$_2$ (Figure 11) and (**Me$_4$dt**)Pt(5′-GMP)$_2$ (Supporting Information) at pH 4.0, the two HT conformers are almost equally abundant, and the HH conformer has a relatively high abundance; these features are unusual when compared to the other **L**Pt(5′-GMP)$_2$ adducts, including the (**5,5′-Me$_2$bipy**)Pt(5′-GMP)$_2$ and (**MepyMe$_2$t**)Pt(5′-GMP)$_2$ adducts studied here. This larger abundance of the HH conformer of the (**R$_4$dt**)Pt(5′-GMP)$_2$ adducts is attributable to the overall low steric effects of the **R$_4$dt** (**R** = Me and Et) ligand.

The chemical shift of the H8 signals and the HH rotamer abundance in (**Et$_4$dt**)Pt(5′-GMP)$_2$, when compared to values for (**Me$_4$dt**)Pt(5′-GMP)$_2$ (Supporting Information), suggest some interaction between the ethyl groups of **Et$_4$dt** and the bound 5′-GMPs. As mentioned above, the 6,6′ ethyl groups impede **G** base rotation. However, at pH 4, the 50% abundance of the HH rotamer for the (**Et$_4$dt**)Pt(5′-GMP)$_2$ adduct was slightly higher than the 40% abundance observed for the (**Me$_4$dt**)Pt(5′-GMP)$_2$ HH rotamer. Thus, the greater bulk of **Et** versus **Me** is reflected primarily in the **G** base rotation rate.

(Et$_4$dt)Pt(3′-GMP)$_2$. The two H8 signals observed in a 2:1 ratio for the (**Et$_4$dt**)Pt(3′-GMP)$_2$ adduct (Figure 15) did not shift when the pH was raised from 4.0 to 7.5. However, the signal at 9.01 ppm became the dominant H8 signal. The CD signal shape at pH 7.5 (Figure 13) is characteristic of the ΔHT conformation.[31,32,43,46] Thus, the 9.01 ppm signal was assigned to the ΔHT conformer, the conformer stabilized by SSC on phosphate deprotonation for 3′-GMP adducts.[35,43,44] The other H8 signal (at 8.87 ppm) is assigned to the ΛHT conformer. The conformer distributions (respective amounts of ΔHT and ΛHT = 67% and 33% at pH 4.0 and 75% and 25% at pH 7.5) are comparable with those for (**Me$_4$dt**)Pt(3′-GMP)$_2$ (Supporting Information).

The HH conformer was not detected for either (**R$_4$dt**)Pt(3′-GMP)$_2$ adduct. The dispersion of the two H8 signals of the (**Et$_4$dt**)Pt(3′-GMP)$_2$ adduct (Table 1) was sufficient for us to resolve an EXSY cross-peak between these H8 signals. The cross-peak confirms that the two observable HT signals are mainly from rapidly interchanging ΔHT and ΛHT conformers; interchange undoubtedly proceeds via the HH conformer (Figure 2). The same exchange process obviously occurs for the (**Me$_4$dt**)Pt(3′-GMP)$_2$ adduct, but the H8 signals are not separated well enough for us to detect the EXSY cross-peak (Supporting Information).

Conclusions

The bulk of the bidentate sp^2 N-donor ligands is sufficient to impede the rotation of the GMPs about the Pt−N7 bonds of the **L**Pt(GMP)$_2$ adducts; thus, H8 signals for conformers could be resolved and assigned. From NMR data (including EXSY results), the qualitative rates of conformer interconversion follow the order **Me$_4$dt** > **Et$_4$dt** > **MepyMe$_2$t** > **5,5′-Me$_2$bipy**.

Thus, we conclude that the pyridyl H6′ atom strongly impedes the rotation of the cis **G** base about the Pt−N7 bond by clashing with **G** O6, whereas the equivalently placed lone pair of the relevant nonbonded N of the triazine does not so strongly impede **G** rotation. Thus, the triazine ring has a lower overall steric effect than the pyridyl ring. The intermediate properties of **MepyMe$_2$t**, with one triazine and one pyridyl ring, led to EXSY data for the (**MepyMe$_2$t**)Pt(5′-GMP)$_2$ adduct that allowed us to unambiguously determine and assign the conformation of the two HH conformers, HHa and HHb.

The nature of both the GMP and the carrier ligand in **L**Pt**G**$_2$ adducts influences the distribution of conformers and their characteristics. The **L**Pt**G**$_2$ adducts studied here have a higher abundance of the HH conformer when **G** = 5′-GMPs than when **G** = 3′-GMPs, supporting the general finding that the 5′-phosphate group stabilizes the HH conformer.[35,44] Typically, one HT conformer dominates over the other HT and the HH conformer at low pH (∼4), especially at neutral pH. We have discovered that carrier ligands of the type **R$_4$dt** lead to the HH having almost comparable abundance to the total of the two HT conformers for the (**R$_4$dt**)Pt(5′-GMP)$_2$ adduct at equilibrium at pH 4. We conclude that the sterically less demanding nature of the **R$_4$dt** ligand allows ample space for the HH conformer to exist with less significant clashes between the O6 atoms of the 5′-GMPs. Normally, second-sphere communication raises the abundance of one H8 conformer as the pH is raised to near neutrality. This trend was found for the (**R$_4$dt**)Pt(5′-GMP)$_2$ adducts. However, the abundance of the HH isomer remains high. Given the finding that carrier ligands favoring the HH conformer in the cross-link are associated with anticancer activity,[16] Pt complexes of **R$_4$dt** ligand should be tested for activity.

In previous studies of **L**Pt(5′-GMP)$_2$ complexes, the CD and NMR spectroscopic data indicate that the ΛHT atropisomer predominates in solution at neutral pH.[19,21,35,43,45,46] The distribution of conformers for the (**5,5′-Me$_2$bipy**)Pt(5′-GMP)$_2$ and (**MepyMe$_2$t**)Pt(5′-GMP)$_2$ adducts agrees with the results for other **L**Pt(5′-GMP)$_2$ adducts. However, the two HT conformers of the (**R$_4$dt**)Pt(5′-GMP)$_2$ (**R** = Me or Et) adducts are unusual in having an approximately equal abundance at low pH and in having an H8 signal for the minor HT form (ΔHT) downfield from that of the major HT form (ΛHT) near physiological pH. At this time, the reason for these differences is not apparent, and additional studies are in progress in order to understand the unique features of (**R$_4$dt**)Pt**G**$_2$ complexes. However, because **R$_4$dt** ligands are sterically less demanding when compared to other sp^2 N-donor ligands, it is possible that steric factors may limit the abundance of the minor HT conformer for **L**Pt(GMP)$_2$ adducts for other **L**'s. Nevertheless, we have made the surprising observation that placing greater bulk at the 6,6′ positions by changing **R** in **R$_4$dt** from Me to Et has a clear effect on the **G** base rotation rate about Pt−N7 bond. We attribute this effect to clashes between the **G** O6 and the methyl group of the 6,6′ ethyl groups (Figure 12).

Finally, our results indicate that adduct formation between **L**PtCl$_2$ (**L** = **5,5′-Me$_2$bipy** and **MepyMe$_2$t**) and 5′- and 3′-GMP does not go to completion, and residual solvated Pt complexes exist at equilibrium. Because the solutions contain DMSO, this solvent both complicates the identification of the solvato species and probably is responsible for incomplete adduct formation. However, this situation presents a rare opportunity to compare the relative binding affinity of 3′-GMP versus 5′-GMP toward Pt(II) in cis bis adducts. The ratio of **L**Pt(3′-GMP)$_2$ to a solvated Pt complex was 46:1 for **L** = **5,5′-Me$_2$bipy** and 38:1 for **L** = **MepyMe$_2$t**, but the ratio of **L**Pt(5′-GMP)$_2$ to a solvated Pt complex was only 5:1 for **L** = **5,5′-Me$_2$bipy** and only 4:1 for **L** = **MepyMe$_2$t**. This greater stability of **L**Pt(3′-GMP)$_2$ compared to **L**Pt(5′-GMP)$_2$ parallels the results observed for the *fac*-[Re(CO)$_3$(H$_2$O)(3′-GMP)$_2$]$^-$ and *fac*-[Re(CO)$_3$(H$_2$O)(5′-GMP)$_2$]$^-$ adducts.[53] This difference in the binding propensity of 3′-GMP versus 5′-GMP is very unlikely to be due to electronic effects because N7 should have very similar donor ability for both 3′-GMP and 5′-GMP. Rather, the difference more likely arises from SSC effects involving the positioning of the phosphate groups. Perhaps the 3′-phosphate group is better positioned to form stabilizing H bonds with N1H of the cis 3′-GMP than is the 5′-phosphate group. Such stabilization of a HT conformer could also explain the generally observed low abundance of the HH conformer of **L**Pt(3′-GMP)$_2$ adducts. The (**5,5′-Me$_2$bipy**)Pt(3′-GMP)$_2$ adduct studied presents an unusual case, in which no HH conformer was detected by using high-field NMR spectroscopy for a 3′-GMP adduct that has rotamers interchanging relatively slowly on the NMR time scale.

Acknowledgment. Instrumentation used in this study was supported by NSF Grant No. 0421356.

Supporting Information Available: Tables listing the chemical shifts of the H1′ and H6/H6′ signals and conformer distribution for **L**Pt(GMP)$_2$ adducts; NMR and CD studies involving (**Me$_4$dt**)-Pt(GMP)$_2$ adducts. This material is available free of charge via the Internet at http://pubs.acs.org.

IC800836T

(53) Adams, K. A.; Marzilli, L. G. *Inorg. Chem.* **2007**, *46*, 4926–4936.